Journal of Inclusion Phenomena and Macrocyclic Chemistry **45:** 109–116, 2003.

New Layered Double Hydroxide, Zn–Ti LDH : Preparation and Intercalation Reactions

OSAMA SABER and HIDEYUKI TAGAYA*

Department of Chemistry and Chemical Engineering, Yamagata University, 4-3-16, Jonan, Yonezawa, Yamagata 992-8510, Japan

(Received 21 March 2002; in final form: 27 September 2002)

Key words: intercalation, layered double hydroxide, organic-inorganic nanohybrid, Zn–Ti LDH

Abstract

The layered double hydroxide (LDH) well known for its ability to intercalate anionic compounds has been prepared conventionally only with bivalent and trivalent cations. In this study, Zn–Ti LDH consisting of bivalent and tetravalent cations was prepared, and reacted with organic monocarboxylic, dicarboxylic and aromatic acids at high or room temperature. XRD patterns of the prepared LDH (Zn–Ti-CO_3) showed that interlayer spacing of the LDH was 0.67 nm. The value was small compared to the usual LDH (Zn–Al–CO_3) of 0.76 nm in the case of carbonate anion as the guest. Also, DTA, TG and DTG analysis indicated that the electrostatic force between the layers and carbonate anions increased where the carbonate anions in Zn–Ti LDH decomposed at 255 °C while those in Zn–Al–CO_3 decomposed at 230–240 °C.

Introduction

An increasing interest exists in layered double metal hydroxides, which are or may be used as catalysts [1–6], photo catalysts, catalyst supports [7, 8], adsorbents [9, 10], anion exchangers [11, 12], medicine [13, 14], and bonding materials. We are interested in the application of layered materials as preferential intercalation of isomers [15–18], and as novel, cost effective, and environmentally friendly separation materials [19–22]. Thermal decomposition of LDH containing carbonate anion gives metal oxides and results in a useful catalyst for a number of peripheral base-catalyzed reactions. A widespread application of LDH is anticipated by reason of the pronounced anion-exchange capacity toward inorganic and organic anions.

LDH constitutes of infinite sheets of brucite-type material charged positively, where divalent cations were replaced in a fraction of x by trivalent cations in octahedral coordination. The general formula for these compounds is $(M2_{1-x}M3_x(OH)_2)^{x+}(A^-)_x \cdot nH_2O$, where M2 and M3 are divalent and trivalent cations, respectively and "A" represents interlamellar anions that restore the electro neutrality of the intercalation compounds. The distance between two adjacent layers depends mainly on the nature of the interlayer species and their electrostatic interaction with the main layers.

The object of this work is to prepare new LDH. This new LDH structure contains bivalent and tetravalent cations in host layers and carbonate anion as the guest (Zn–Ti–CO_3). This may lead to changes in the characteristics of LDH structure and gives new formulae where the electrostatic interactions between layers and anions increase.

Experimental

Materials

The Zn–Ti LDH was prepared by co-precipitation of zinc and titanium salts from homogeneous solution. A solution of zinc chloride (5.94×10^{-2} mole) and titanium chloride (9.50×10^{-3} mole) were mixed with urea solution under vigorous stirring and heating. The percentage of titanium is 14 mole%. After filtration and washing several times in distilled water, the products were dried at 90 °C for 12 h. Zn–Al–CO_3 LDH was prepared also by the same method for comparison.

The sodium salts of dicarboxylic acids (glutaric, suberic, sebacic and dodecanedioic acids) and some monocarboxylic acids (hexanoic, palmitic and behenic acids) were prepared by neutralization of the corresponding organic acids with sodium hydroxide. All organic acids and sodium salts of monocarboxylic acids and aromatic acids were obtained from WAKO and T.C.I. (Tokyo).

Intercalation

Typically, the appropriate amount of organic acid sodium salt (0.002 mole) dissolves in 10 ml of deionized–distilled water (concentration about 0.2 M) with ultrasonic treatment.

The LDH (0.24 g) was mixed with the solution of organic acid under Ar atmosphere and stirred at room temperature

* Author for correspondence.

for 72 h or at 60 °C for 6 h. After filtration and washing, the samples were dried under vacuum at room temperature.

Characterization

Powder X-ray diffraction (XRD) spectra were recorded on Rigaku, RINT 2200 using CuKα (filtered) radiation (λ = 0.154 nm) at 40 kV and 20 mA between 1.8 and 50°. Thermal analyses (TG, DTG and DTA) of powdered samples up to 800 °C were carried out at a heating rate of 10 °C/min in the flow of nitrogen gas using a Seiko SSC 5200 apparatus. FT-IR spectra (KBr disc method) were recorded on a Horiba FT-720. Scanning electron microscopy (SEM) was performed with JEOL, JSM-6330F, (15 kV/12 mA).

Results and discussions

Chemical analysis of Zn–Ti–CO_3 LDH

The chemical analysis of Zn–Ti–CO_3 LDH indicates that the percentage of carbon and hydrogen are 3.71 and 1.25, respectively. After the intercalation of *n*-capric acid, the percentage of carbon and hydrogen increased to 21.86 and 3.97, respectively. These results confirm that the Zn–Ti–CO_3 LDH accept the intercalation reactions. Electron spectroscopy for chemical analysis (ESCA) supported the presence of titanium in the solid as tetravalent cation. Whereas, the electron binding energy of Ti (2p) for Zn–Ti–CO_3 LDH is 464.05 eV and was value coincident with 464.8 eV of TiO_2 in Shimadzu ESCA Data [23].

Elemental chemical analysis (as determined by ICP) for Zn–Ti–CO_3 LDH shows that the Zn^{2+}/Ti^{4+} mole ratio is about 10. This means that there are some deviations compared with 6.3 of the mole ratio existing in the starting solution. The lack of coincidence between the initial ratio of cations in the solution and the ratio in the solid isolated, is, however, rather common [24, 25] and may be ascribed to a preferential precipitation of one or another cation as hydroxide or error during measurement.

X-ray diffraction

The X-ray diffraction of Zn–Ti–CO_3 LDH (Figure 1a) showed the basal peaks of planes hkl (003), (006) and (009) and non-basal peaks (100), (101), (012) and (104) with little shifting for basal peaks to higher scattering angles (2θ) compared with natural and synthetic hydrotalcites [1, 26–28].

This indicates that the thickness of the unit layer (d_{003}) decreases with the incorporation of tetravalent metal instead of trivalent metal in hydrotalcite materials. Gastuche *et al.* [26, 29] showed that the non-basal reflections in synthetic hydrotalcite at d = 0.273, 0.265, 0.259 and 0.246 nm were considered to be relative to the (100), (101), (012) and (104) planes and the presence of both sharp and diffuse non-basal reflection was taken as an indication of a partially disordered structure.

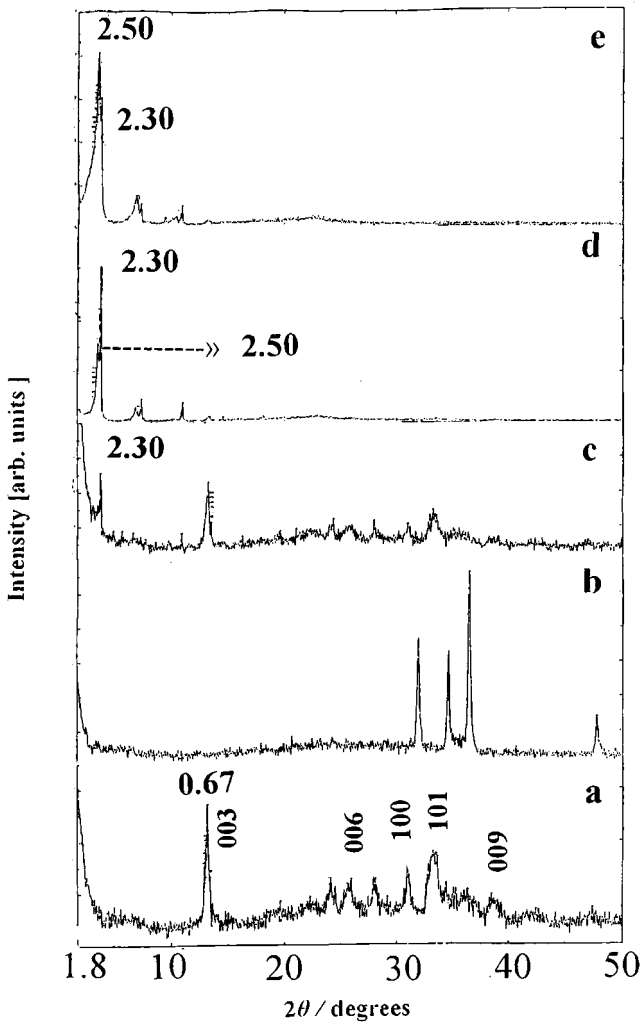

Figure 1. X-ray diffraction patterns of (a) Zn–Ti–CO_3 LDH, (b) Zn–Ti LDH after calcinations at 500 °C, and Zn–Ti LDH after intercalation of *n*-capric acid in (c) low concentration at 60 °, (d) high concentration at 60 °, and (e) high concentration at r.t.

A weak reflection at d = 0.36 and 0.32 nm is observed. We assign those reflections as those due to impurities of zinc hydroxide [30].

The XRD pattern of Zn–Ti–CO_3 LDH has the main peak at 0.67 nm which corresponded to interlayer spacing of the LDH, as shown in Figure 1a. The peaks exhibit some common features of layered materials such as narrow, symmetric, strong peaks at low 2θ values and weaker, less symmetric peaks at high 2θ values. The peak at 0.67 nm disappeared by the calcination at 500 °C. The appearance of new peaks at high 2θ values, as shown in Figure 1b, indicates the formation of metal oxides. By the reaction of Zn–Ti LDH with *n*-capric acid, clear new peaks were observed, as shown in Figures 1c, d, and e.

Interlayer spacing, 0.67 nm of Zn–Ti–CO_3 LDH, was small compared to 0.76 nm of Zn–Al–CO_3 LDH. Pinnavaia [31] and Yun *et al.* [32] have reported that interlayer spacing, 0.76 nm, of the LDH consisting of bivalent and trivalent cations, decreased to 0.67 nm by drying at 150 °C. The process was considered as the desorption process of water in space between layers. In Zn–Ti–CO_3 LDH, titanium

Table 1. Intercalation of organic acids into Zn–Ti LDH

Guest	Guest (mol%)	Time (h)	Temp. (°C)	Peaks in XRD (nm)
Monocarboxylic acid				
$CH_3(CH_2)_4COOH$	0.0027	72	r.t.	1.54, 0.79, 0.53, 0.43
$CH_3(CH_2)_8COOH$	0.0015	5	60	2.3, 0.81, 0.67
$CH_3(CH_2)_8COOH$	0.002	5	60	2.5, 2.3, 1.3, 1.2, 0.8
$CH_3(CH_2)_8COOH$	0.002	72	r.t.	2.5, 2.3, 1.3, 1.2, 0.8
$CH_3(CH_2)_{12}COOH$	0.002	72	r.t.	3.4, 3.0, 2.8, 1.8, 1.6, 1.5, 1.1, 1.0
$CH_3(CH_2)_{12}COOH$	0.0012	5	60	3.4, 2.8, 1.8, 1.5, 1.2
$CH_3(CH_2)_{14}COOH$	0.002	72	r.t.	3.4, 1.8, 1.2, 0.9, 0.75
$CH_3(CH_2)_{16}COOH$	0.002	72	r.t.	4.3, 3.8, 3.4, 2.0, 1.7, 1.6, 1.3, 1.2
$CH_3(CH_2)_{16}COOH$	0.0008	5	60	3.98, 3.2, 1.8, 1.5, 1.2
$CH_3(CH_2)_{20}COOH$	0.002	72	r.t.	4.55, 2.39, 1.6, 1.2, 1.0
Dicarboxylic acid				
$HOOC(CH_2)_3COOH$	0.002	5	60	0.68, 0.67, 0.38, 0.34
$HOOC(CH_2)_6COOH$	0.002	5	60	1.04, 0.52, 0.43
$HOOC(CH_2)_8COOH$	0.002	5	60	1.21, 0.61, 0.45, 0.38, 0.29
$HOOC(CH_2)_{10}COOH$	0.002	5	60	1.42, 0.72, 0.67, 0.45
Aromatic acid				
4-chlorophthalic acid	0.002	5	60	1.64, 0.69, 0.51, 0.47, 0.43, 0.31

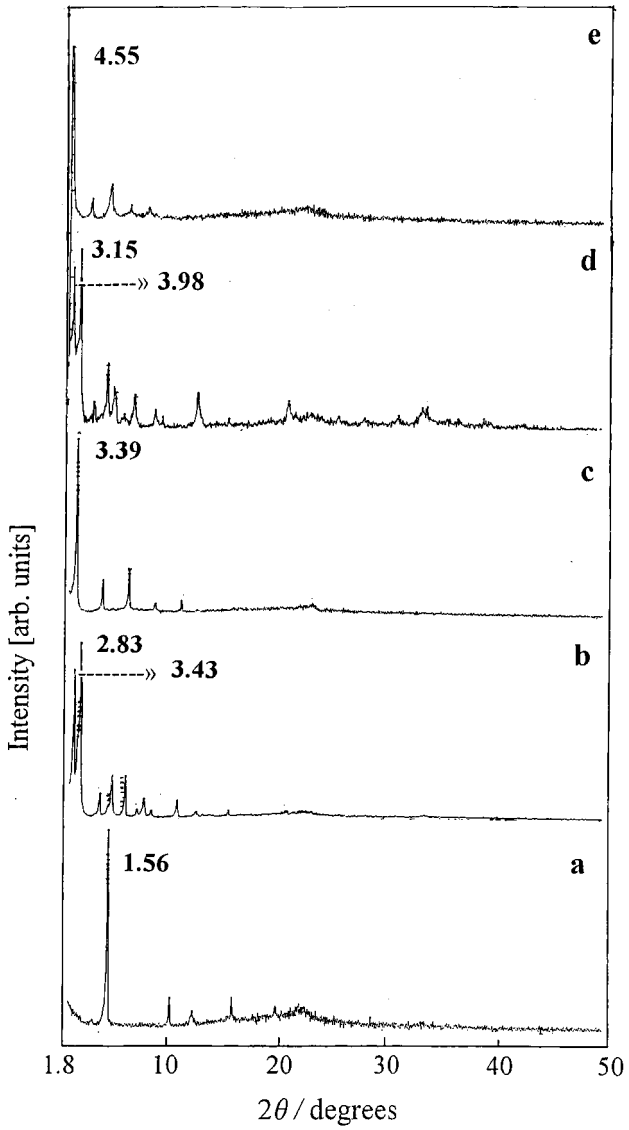

Figure 2. X-ray diffraction patterns of reaction products of Zn–Ti–CO_3 LDH with (a) hexannoic acid ($CH_3(CH_2)_4COOH$), (b) myristic acid ($CH_3(CH_2)_{12}COOH$), (c) palmitic acid ($CH_3(CH_2)_{14}COOH$), (d) stearic acid ($CH_3(CH_2)_{16}COOH$), and (e) behenic acid ($CH_3(CH_2)_{20}COOH$).

cation replaced zinc cation indicating that a positive charge (+2) was produced. There is a possibility that the electrostatic force between inorganic layer and guest compounds is stronger than that in the case of Zn–Al LDH.

This speculation is supported by the comparison of the thermal characteristics of Zn–Ti LDH with Zn–Al LDH, as described later.

By the treatment of Zn–Ti–CO_3 with an aqueous solution of *n*-capric acid (0.0015 mol) at 60 °C, a new peak was observed at 2.3 nm, as shown in Figure 1c. In the treatment with an aqueous solution of *n*-capric acid (0.002 mol), the peak at 2.3 nm became sharper and the peak of LDH itself (0.67 nm) disappeared, as shown in Figure 1d, suggesting complete intercalation. The intercalation reaction occurred also at room temperature, as shown in Figure 1e.

The interlayer anions of the LDH (carbonate ion) were also exchanged by various aliphatic acids whose carbon numbers were 6, 14, 16, 18, and 22 at room temperature or at high temperature.

The interlayer spacing of the LDH increased to 1.56 nm when hexanate anion whose carbon number was 6 was exchanged, as shown in Figure 2a. Certainly, interlayer spacing of the LDH increased with the chain length of aliphatic acids, as shown in Table 1, by the reaction of LDH with monocarboxylic acid.

The XRD patterns of intercalation compounds showed that they have one or two sharp peaks at low 2θ values, depending on the concentration and kinds of acids, as shown in Figure 2. The interlayer spacing increased from 2.3 nm, whose guest was *n*-capric acid to 4.55 nm, whose guest was behenic acid. These values agreed well with those reported by Meyn *et al.* [12].

In the reaction of Zn–Ti LDH with dicarboxylic acids, whose carbon numbers were 5 to 12, interlayer spacing increased, as shown in Figure 3, although a small peak at 0.67 was also observed. The interlayer spacing of the dicarboxylic acid intercalation compounds increased linearly with the chain length of dicarboxylic acids, as shown in Figure 4. The mean increment of interlayer spacing was 0.101 nm/CH_2 carbon. This agreed with the results previously published in the case of divalent-trivalent LDH [12, 13].

As the approximate thickness of the brucite layer is 0.48 nm, the interlayer heights generated are close to 0.20 nm, 0.52 nm, 0.72 nm and 0.96 nm, for acids whose carbon number were 5, 8, 10 and 12, respectively. It sug-

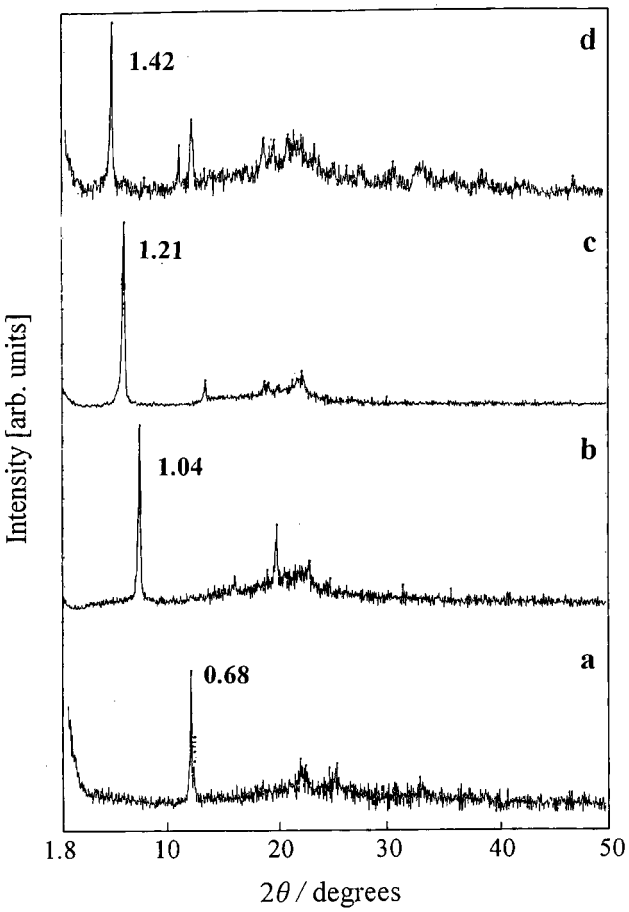

Figure 3. X-ray diffraction patterns of reaction products of Zn–Ti–CO_3 LDH with (a) glutaric acid ($COOH(CH_2)_3COOH$), (b) suberic acid ($COOH(CH_2)_6COOH$), (c) sebacic acid ($COOH(CH_2)_8COOH$), and (d) dodecanedioic acid ($COOH(CH_2)_{10}COOH$).

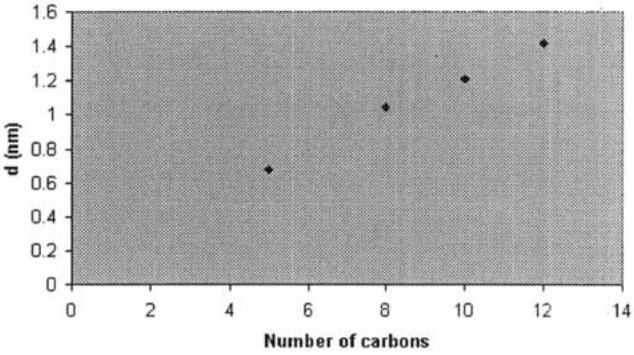

Figure 4. The effect of carbon numbers of intercalated dicarboxylic acids on interlayer spacings (nm) of Zn–Ti LDH.

gested that the anion is lying perpendicular, tilting with the layers.

Table 1 also listed the interlayer spacing of LDH intercalation compound of aromatic acid. In the reaction with 4-chloro phthalic acid, interlayer spacing increased to 1.64 nm. This indicates that the intercalation of aromatic acids is also possible into Zn–Ti LDH. From these XRD patterns, we can expect the orientation of carbonate anions between Zn–Ti LDH layers, as shown in Figure 5.

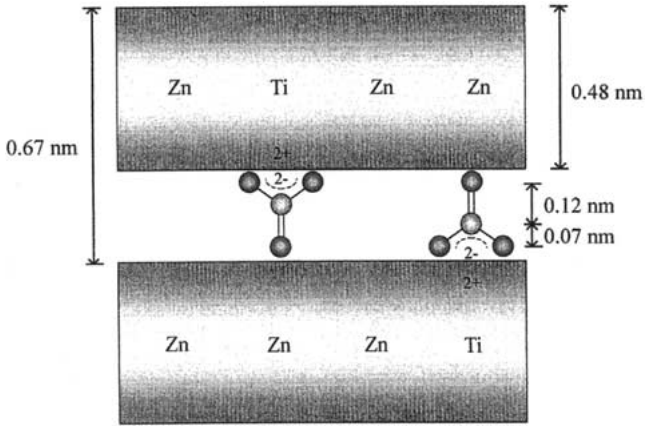

Figure 5. Schematic representation of Zn–Ti–CO_3 LDH.

Thermal analysis

Thermal characteristics of the LDH were determined by TG, DTG and DTA, as shown in Figure 6. The comparison of Zn–Ti LDH with Zn–Al LDH in TG and DTG diagram showed that the weight loss for Zn–Al LDH up to 200 °C, is 7%, whilst the weight loss for Zn–Ti LDH up to the same temperature, is only 1.7%. This means that the amount of interlayer water of Zn–Ti LDH is small compared to Zn–Al LDH. There is a possibility that the interlayer space of Zn–Ti LDH is smaller than that of Zn–Al LDH, and Zn–Ti LDH has no sufficient space for water. The main weight loss occurs from 200 °C to 279 °C that corresponded to the evaporation of carbonate anions.

DTA diagram show that Zn–Al LDH has three endothermic peaks, as shown in Figure 6a. The first broad peak at around 130 °C corresponds to the desorption of surface and interlayer water, the second sharp peak at 231 °C corresponds to the decomposition of carbonate anions and the third small peak at 259 °C corresponds to the dehydroxylation of layers.

However, in the case of Zn–Ti LDH, only one sharp peak was observed at 256 °C, as shown in Figure 6b. This peak corresponded to desorption of carbonate anions and the dehydroxylation process. These results suggested that the carbonate anions in Zn–Ti LDH have stronger interaction with brucite layers than those in Zn–Al LDH. This suggestion agreed with small interlayer spacing of Zn–Ti LDH compared to Zn–Al LDH.

TG curves of monocarboxylic acids and Zn–Ti intercalation compounds of the acids are shown in Figure 7. Decomposition temperature of monocarboxylic acids shifted to higher temperature by intercalation. These TG analyses agreed with DTA data.

Figure 8 showed the DTA curves of dicarboxylic acids and Zn–Ti intercalation compounds of the acids. These results also suggested occurrence of the intercalation reaction and the presence of some carbonate anions in the interlayer space. The decomposition temperatures of suberic acid and sebacic acid were 279 °C and 286 °C, respectively. The temperatures shifted to 376 °C and 397 °C, respectively, by

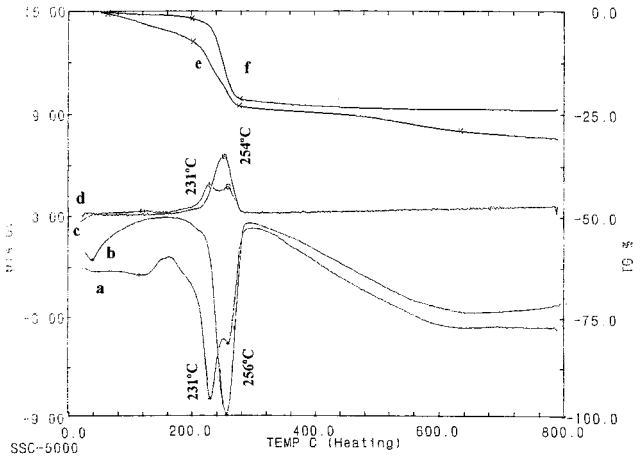

Figure 6. TG, DTG and DTA of Zn–Ti–CO_3 LDH (curves b, d and f) and Zn–Al–CO_3 LDH (curves a, c and e).

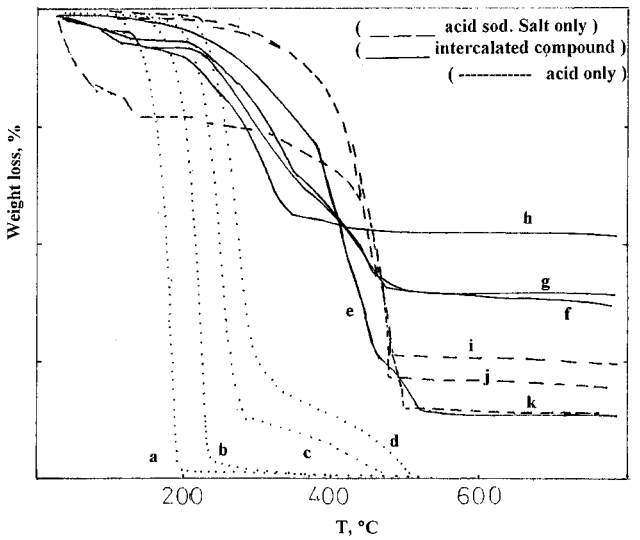

Figure 7. Thermal analyses (TG) of (a) *n*-capric acid, (b) myristic acid, (c) stearic acid, (d) behenic acid, and the reaction product of Zn–Ti LDH-CO_3 with (e) behenic acid sodium salt, (f) stearic acid sodium salt, (g) myristic acid sodium salt, (h) *n*-capric acid sodium salt, and (i) *n*-capric acid sodium salt alone, (j) myristic acid sodium salt alone and (k) stearic acid sodium salt alone.

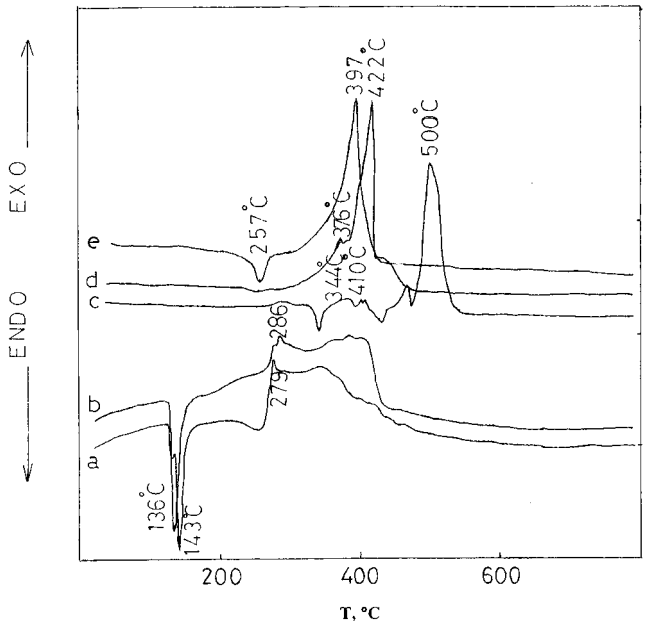

Figure 8. Differential thermal analysis (DTA) of (a) suberic acid ($COOH(CH_2)_6COOH$), (b) sebacic acid ($COOH(CH_2)_8COOH$), and the reaction product of Zn–Ti–CO_3 LDH with (c) suberic acid, (d) sebacic acid, (e) glutaric acid.

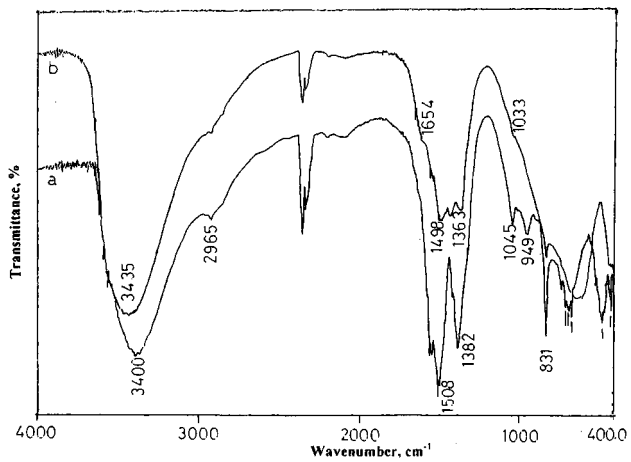

Figure 9. IR spectra of (a) Zn–Ti LDH and (b) Zn–Al LDH.

intercalation. The peak at 257 °C corresponded to the weight loss by the decomposition of carbonate anions.

FT-IR spectroscopy

The FT-IR technique has been used to identify the nature and symmetry of interlayer anions. FT-IR spectra of Zn–Al LDH and Zn–Ti LDH are similar, as shown in Figure 9.

Two patterns showed broad intense bands between 3600 and 3300 cm^{-1} due to the OH stretching mode of layer hydroxyl groups and of interlayer water molecules. OH band for Zn–Ti LDH was 3400 cm^{-1} compared to 3435 cm^{-1} of that for Zn–Al LDH. This shift may depend on the nature of the layer cation, as its electro-negativity will modify the electron density on the O–H bond (M–OH) and the extreme broadness of the OH band may be owed to the presence of hydrogen bonding [1, 33, 34].

A weak shoulder peak recorded at around 3000 cm^{-1} has been ascribed to the OH stretching mode of interlayer water molecules, hydrogen-bonded to interlayer carbonate anions [35, 36]. The bending mode band of water molecules, usually observed close to 1600 cm^{-1} [37], is recorded only as a weak shoulder on the large wavenumber side of the stretching band at 1500 cm^{-1} in the case of Zn–Al LDH, while in the case of Zn–Ti LDH, no band was observed in this position. This may mean that the amount of interlayer water inside Zn–Ti LDH is small. This speculation was supported by the results of XRD, DTA and TG.

The band at 1508 cm^{-1} together with its companion band at 1382 cm^{-1}, should be due to mode ν_3 of interlayer carbonate species [35, 38]. This band is recorded at 1450 cm^{-1} for free carbonate species, but it splits and shifts upon a symmetry lowering. So, for aragonite, it is known that it splits into two bands at 1504 and 1492 cm^{-1}. In the

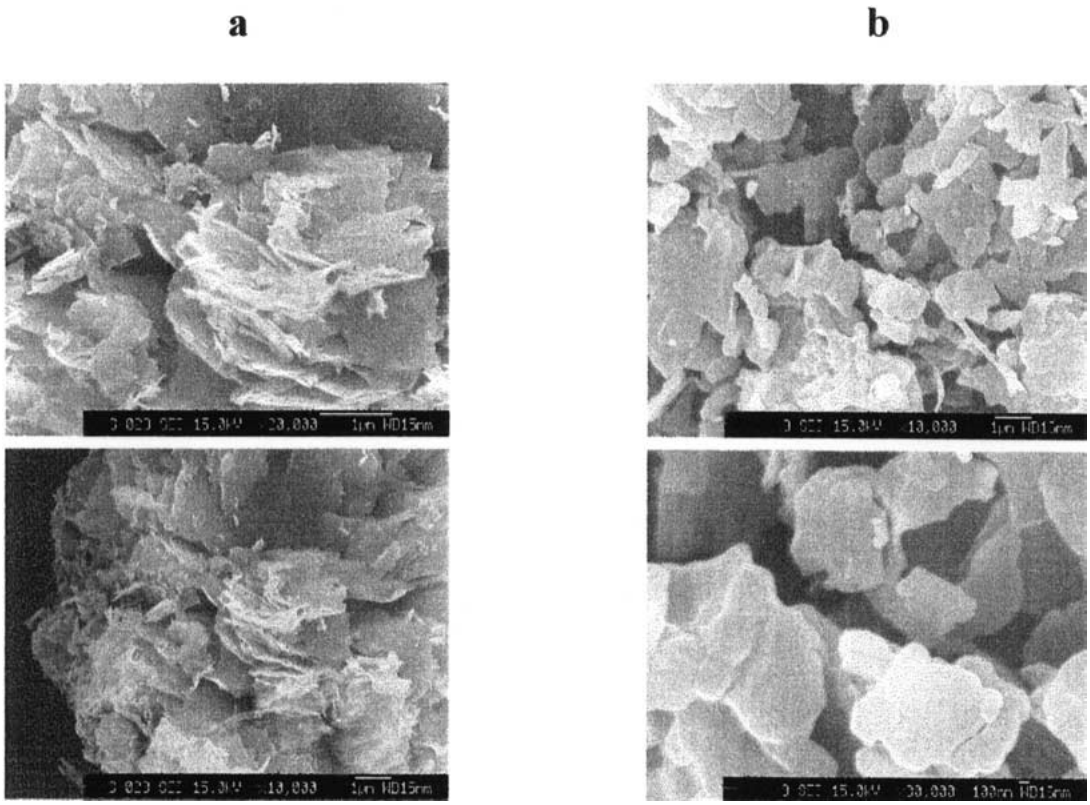

Figure 10. SEM images of (a) Zn–Ti–CO_3 LDH and (b) reaction products of Zn–Ti–CO_3 LDH with stearic acid.

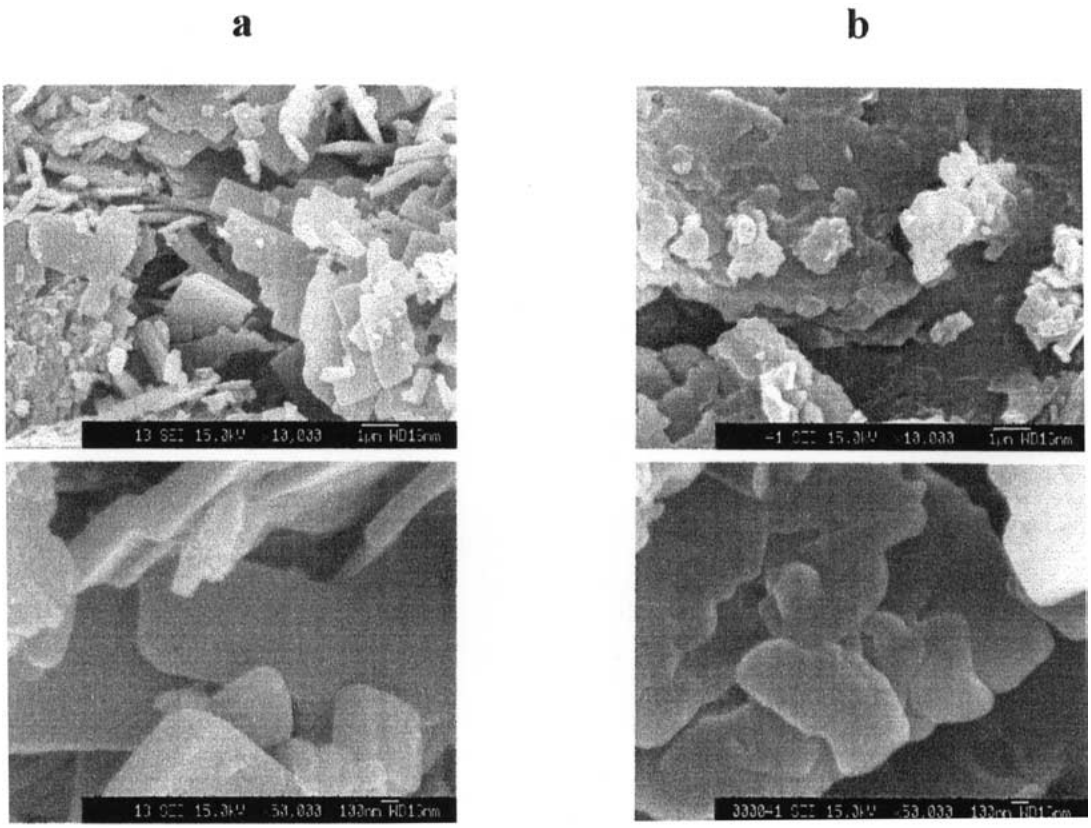

Figure 11. SEM images of the reaction products of Zn–Ti–CO_3 LDH with (a) sebacic acid and (b) behenic acid.

present case, the splitting is similar, probably due to the restricted symmetry in the interlayer space, in addition to the different electrostatic interactions because of the distortions originated by the two, different size cations in the layers.

The weak band observed at 1045 cm^{-1} for Zn–Ti LDH can be ascribed to the ν_1 mode of carbonate. Although this band is IR-inactive in the free carbonate, it becomes activated owing to the lowering of the symmetry of carbonate anion in the interlayer, which is also responsible for the splitting of the ν_3 band [39]. This band is also observed in Zn–Al LDH as a weak shoulder at 1033 cm^{-1}.

The sharp bands observed at below 1000, 949 and 831 cm^{-1} could be ascribed to mode ν_2 of carbonate anion. Bands at 879 and 866 cm^{-1} are those for free ion and aragonite, respectively. Mode ν_4 of carbonate anion could be responsible for bands at 690 and 707 cm^{-1}. The band at 706 cm^{-1} is for free carbonate anion and the band splits into two bands at 711 and 706 cm^{-1} for aragonite [35, 38].

These results indicate that the prepared Zn–Ti LDH has a similar structure with the usual Zn–Al LDH structure and it confirmed the presence of carbonate anions and small amount of water inside the interlayer space. Also, the existence of organic compounds into Zn–Ti LDH were confirmed by the results of IR spectroscopy.

Scanning electron microscope (SEM)

SEM images of Zn–Ti LDH before and after intercalation of organic compounds are shown in Figures 10 and 11. Zn–Ti LDH and the intercalation compounds have a clear plate-like morphology, which was typical for the LDH morphology. Also, the images indicated that the average size of the organic compounds containing crystallites is much larger than that of the samples before intercalation reactions. This was also supported by the results of XRD and TG.

Discussion

For Zn–Ti–CO_3 LDH, interlayer spacing was calculated from the thickness of the Brucite layer and the size of the carbonate ion, as shown in Figure 5. The observed spacing, 0.67 nm, agrees thoroughly with the calculated value. Pinnavaia [31] and Yun *et al.* [32] have reported that basal spacing of the Mg–Al–CO_3 LDH decreased to 0.67 nm after drying at 150 °C, i.e., after removing interlayer surface water. The interlayer spacing agreed with the basal spacing of Zn–Ti LDH and also suggested the presence of a small amount of interlayer water.

The most remarkable behavior of Zn–Ti LDH is the high reactivity toward various types of organic anions, such as monocarboxylic-, dicarboxylic-aliphatic acids and aromatic acids. Also, the intercalation reactions do not depend strongly on the alkyl chain length, i.e., Zn–Ti LDH allowed intercalation reaction of acids not only having short methylene chain length, but also large methylene chain length.

The experimental results show that the fatty acids such as stearate anion are intercalated into the interlayer spacing and bound to the host matrix by electrostatic force with two interlayer spacing, 3.98 and 3.15 nm. The powder XRD patterns are not sufficiently high quality to allow us to carry out structure determination. However, from interlayer spacing and the size of the guest ions, orientation of guest ions was considered. From known layer thickness, 0.48 nm, the interlayer spacing available for the anion were calculated as 3.5 nm and 2.64 nm. By comparison with the size of stearate anion, 2.25 nm, it was considered that the intercalation compound has two orientations, monolayer and bilayer structures. Whereas XRD patterns indicated that some kinds of fatty acids such as acids having carbon number, 6, 10, 16 and 22, make a bilayer structure only. The formation of the bilayer structure can be explained by hydrophobic interaction between stearate molecules. This means that the main structure for all fatty acids is a bilayer structure and this consideration agrees with structures reported by Takagi *et al.* [40]. In the intercalation of dicarboxylic acids, a bridging structure between the layers was suggested from interlayer spacing and the size of dicarboxylic acids.

Conclusions

In this study, layered double hydroxide consisting of bivalent and tetravalent cations has been prepared for the first time. The Zn–Ti–CO_3 LDH has small interlayer spacing, 0.67 nm, compared to usual Zn–Al–CO_3 LDH. Anion-exchange reactions were successful in replacing the carbonate anions with monocarboxylate, dicarboxylate and phthalate anions. The preparation and characterization of Zn–Ti-organic anion LDH have been clarified in this study.

References

1. F. Cavani, F. Trifiro and A. Vaccari: *Catal. Today* **11**, 173 (1991).
2. S.P. Newman and W. Jones: *New J. Chem.* **22**, 105 (1998).
3. T. Takatsuka, H. Kawasaki, S. Yamashita and S. Kohjiya: *Bull. Chem. Soc. Jpn.* **52**, 2449 (1979).
4. S. Kohjiya, T. Sato, T. Nakayama and S. Yamashita: *Macromol. Rapid Commun.* **2**, 231 (1981).
5. W.T. Reichle: *J. Catal.* **94**, 547 (1985).
6. E. Suzuki and Y. Ono: *Bull. Chem. Soc. Jpn.* **61**, 1008 (1988).
7. H. Schaper, J.J. Berg-Slot and W.H.J. Stork: *Appl. Catal.* **54**, 79 (1989).
8. L. Barloy, J. P. Lallier, P. Battioni, D. Mansuy, Y. Piffard, M. Tournoux, J. B. Valim and W. Jones: *New J. Chem.* **16**, 71 (1992).
9. P.C. Pavan, G.D. Gomes and J.B. Valim: *Microporous Mesoporous Mater.* **21**, 659 (1998).
10. P.C. Pavan, E.L. Crepaldi, G.D. Gomes and J.B. Valim: *Colloids Surf. A* **154**, 399 (1999).
11. S. Miyata and T. Kumura: *Chem. Lett.* 843 (1973).
12. M. Meyn, K. Beneke and G. Lagaly: *Inorg. Chem.* **29**, 5201 (1990).
13. A. Schmassmann, A. Tarnawski, B. Flogerzi, M. Sanner, L. Varga and F. Halter: *Eur. J. Gastroenterol. Hepatol.* **5**, S111 (1993).
14. J. Choy, S. Kwak, J. Park, Y. Jeong and J. Portier: *J. Am. Chem. Soc.* **121**, 1399 (1999).
15. A. Fogg, V. Green, H. Harvey and D. O'Hare: *Adv. Mater.* **11**, 1466 (1999).
16. H. Tagaya, S. Ogata, S. Nakano, J. Kadokawa, M. Karasu and K. Chiba: *J. Inclusion Phenomena* **31**, 231 (1998).
17. S. Ogata, H. Tagaya, M. Karasu, J. Kadokawa and K. Chiba: *Trans. MRS-J.* **24**, 501 (1999).

18. S. Ogata, H. Tagaya, M. Karasu and J. Kadokawa: *J. Mater. Chem.* **10**, 321 (2000).
19. T. Takahashi, H. Adachi, J. Kadokawa and H. Tagaya: *Trans. Mater Res. Soc. Jpn.* **26**(2), 491 (2001).
20. H. Tagaya, S. Sato, T. Kuwahara, J. Kadokawa, M. Karasu and K. Chiba: *J. Mater. Chem.* **4**, 1907 (1994).
21. H. Tagaya, A. Ogata, T. Kuwahara, S. Ogata, M. Karasu, J. Kadokawa and K. Chiba: *Microporous Materials* **7**, 151 (1996).
22. H. Tagaya and S. Ogata: *Function and Material* **18**, 33 (1998).
23. Shimadzu ESCA Data: ESCA 750.
24. A. Roy, C. Forano, K. Elmalki and J. Besse: in M. L. Occelli and H. Robson (eds.), *Expanded Clay and other Microporous Solids, Synthesis of Microporous Materials*, V. Reinhold, New York, Ch. 7, p. 108 (1992).
25. V. Rives and S. Kannan: *J. Mater. Chem.* **10**, 489 (2000).
26. M.C. Gastuche, G. Brown and M. Mortland, *Clay Minerals* **7**, 72 (1967).
27. C. Busetto, G. Del Piero, and G. Manara: *J. Catal.* **85**, 260 (1984).
28. R. Allmam and H.H. Lohse: *N. Jhb. Miner. Mh.* **6**, 161 (1966).
29. F. Leroux, M. Adachi-Pagano, M. Intissar, S. Chauviere, C. Forano and J. Besse: *J. Mater. Chem.* **11**, 105 (2001).
30. JCPDS file No. 20-1437.
31. Constantino and T. Pinnavaia: *Inorg. Chem.* **34**(4), 883 (1995).
32. S. Yun and T. Pinnavaia: *Chem. Mater.* **7**, 348 (1995).
33. A. Vaccari: *Appl. Clay Sci.* **14**, 161 (1999).
34. F.M. Labajos, V. Rives and M.A. Ulibarri: *J. Mater. Sci.* **27**, 1546 (1992).
35. S. Miyata: *Clays Clay Miner.* **23**, 369 (1995).
36. E.C. Kruissink, L.L. Van Reijden and J.R.H. Ross: *J. Chem. Soc., Faraday Trans. 1* **77**, 649 (1991).
37. J. Perez-Ramirez, G. Mul, F. Kapteijn and J.A. Moulijn: *J. Mater. Chem.* **11**, 821 (2001).
38. N. Nakamoto: *Infrared and Raman Spectra of Inorganic and Coordination Compounds*, 4th edn., John Wiley & Sons, New York (1986).
39. M.K. Titulaer, J.B.H. Jansen and J.W. Geus: *Clays Clay Miner.* **42**, 249 (1994).
40. T. Kanoh, T. Shichi and K. Takagi: *Chem. Lett.* 117 (1999).